



Twin-variant reorientation-induced large magnetoresistance effect in Ni₅₀Mn₂₉Ga₂₁ single crystal

Min Zeng, Siu Wing Or, Zhiyong Zhu, and S. L. Ho

Citation: J. Appl. Phys. **108**, 053716 (2010); doi: 10.1063/1.3480794

View online: <http://dx.doi.org/10.1063/1.3480794>

View Table of Contents: <http://jap.aip.org/resource/1/JAPIAU/v108/i5>

Published by the American Institute of Physics.

Related Articles

Large amplitude microwave emission and reduced nonlinear phase noise in Co₂Fe(Ge_{0.5}Ga_{0.5}) Heusler alloy based pseudo spin valve nanopillars
Appl. Phys. Lett. 99, 162508 (2011)

Proper scaling of the anomalous Hall effect in the Co/Pt multilayers
J. Appl. Phys. 110, 033921 (2011)

Physical nature of anomalous peaks observed in extraordinary Hall effect measurement of exchange biased spin-valves with perpendicular anisotropy
J. Appl. Phys. 110, 013913 (2011)

Existence of modulated structure and negative magnetoresistance in Ga excess Ni-Mn-Ga
Appl. Phys. Lett. 99, 021902 (2011)

Thermoelectric properties of Ga-added CoSb₃ based skutterudites
J. Appl. Phys. 110, 013521 (2011)

Additional information on J. Appl. Phys.

Journal Homepage: <http://jap.aip.org/>

Journal Information: http://jap.aip.org/about/about_the_journal

Top downloads: http://jap.aip.org/features/most_downloaded

Information for Authors: <http://jap.aip.org/authors>

ADVERTISEMENT


AIP Advances

Submit Now

**Explore AIP's new
open-access journal**

- **Article-level metrics
now available**
- **Join the conversation!
Rate & comment on articles**

Twin-variant reorientation-induced large magnetoresistance effect in $\text{Ni}_{50}\text{Mn}_{29}\text{Ga}_{21}$ single crystal

Min Zeng, Siu Wing Or,^{a)} Zhiyong Zhu, and S. L. Ho

Department of Electrical Engineering, The Hong Kong Polytechnic University, Hung Hom, Kowloon, Hong Kong

(Received 5 May 2010; accepted 19 July 2010; published online 14 September 2010)

We report a significant magnetoresistance (MR) effect arisen from magnetic field-induced reorientation of martensitic twin variants in a ferromagnetic shape memory $\text{Ni}_{50}\text{Mn}_{29}\text{Ga}_{21}$ single crystal. The measured electrical resistivity shows large anisotropy and the measured MR value is as large as 25% over the wide temperature range of 230-315 K at a moderate magnetic field of 1.2 T. It is found that a proper combination of the initial state of martensitic twin variants and the direction and magnitude of applied magnetic field can give rise to either positive or negative MR value of $\sim 25\%$, thus allowing a periodic modulation of the MR effect in response to varying the spatial angle between the directions of applied magnetic field and electric current for every 180° . © 2010 American Institute of Physics. [doi:10.1063/1.3480794]

I. INTRODUCTION

Since the discovery of giant magnetoresistance (GMR) in Fe/Cr multilayers,¹ the study of magnetoresistance (MR) effect in magnetic materials has been greatly intensified in recent years for potential applications in magnetic heads and data storages.²⁻⁶ In fact, the MR effect in different materials can have different underlying mechanisms. For instances, spin-dependent scattering of conduction electrons is responsible for GMR in magnetic multilayers and granular thin films,¹⁻⁴ while modification of electronic band structure by magnetic field-induced first-order magnetic and/or crystal-phase transition is in charge of MR in some bulk intermetallic compounds.^{5,6}

More recently, the MR effect has been observed in some half-metallic Heusler alloys with the general formula $\text{Ni}_2\text{Mn}_{1+x}\text{X}_{1-x}$ (where X is a *sp*-element such as Sn, Sb, In, etc.) and in some Heusler-type ferromagnetic shape memory alloys (such as Ni-Mn-Ga alloys).⁷⁻¹² In particular, the reported MR effect in these Heusler alloys is basically in polycrystalline bulks and thin films with either positive or negative MR value, depending on applied magnetic field and (low) temperature. It is argued that the underlying mechanisms are mainly governed by the *s-d* scattering for the bulks and the spin transport for the thin films.^{10,11}

Among the Heusler alloys, Ni-Mn-Ga single crystals exhibit giant magnetic field-induced strains (MFISs) of $\sim 6\%$ (load-free) in the tetragonal martensitic phase and of $\sim 10\%$ in the orthorhombic martensitic phase as a result of the martensitic twin-variant reorientation induced by magnetic field, mechanical stress, and/or temperature.¹³⁻¹⁵ This reorientation may also lead to a characteristic change in electrical resistivity due to crystallographic anisotropy.¹⁶ Here, it turns to a physically interesting and technologically important question, i.e., whether the reorientation of martensitic twin vari-

ants in the single crystals can also induce an MR effect or not. Such an issue would be especially crucial to exploring the multifunctionality of the single crystals.

In this work, we investigate the MR effect in a $\text{Ni}_{50}\text{Mn}_{29}\text{Ga}_{21}$ single crystal over a broad temperature range from 230 to 315 K, which covers the room temperature (298 K). Our experiments reveal both positive and negative MR effects, each of $\sim 25\%$ in magnitude, in response to a relatively low magnetic field of 1.2 T. Besides, the underlying mechanism for such interesting effects, which is essentially different from other mechanisms proposed so far, is the reorientation of martensitic twin variants induced by magnetic field plus the electrical resistivity anisotropy.

II. EXPERIMENTAL DETAILS

Plate-shaped $\text{Ni}_{50}\text{Mn}_{29}\text{Ga}_{21}$ single crystal, with dimensions of $11.500(l) \times 3.221(w) \times 0.487(t)$ mm³ (where *l* = length, *w* = width, and *t* = thickness), crystallographic orientations of [001], [100], and [010] along the *l*-, *w*-, and *t*-directions, respectively, and a load-free MFIS of 5.6% at room temperature, was supplied by AdaptaMat Ltd. in Finland. Figure 1 illustrates the schematic diagram of the single crystal, detailing its crystallographic orientations and the directions of applied magnetic field (*H*) and electric current (*I*), according to the three-dimensional Cartesian coordinate system. The single crystal in the martensitic phase was deter-

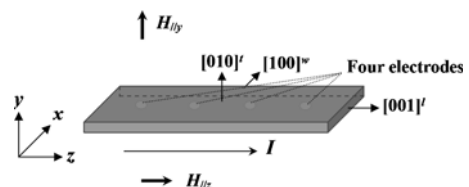


FIG. 1. (Color online) Schematic diagram of the single crystal, showing its crystallographic orientations and the directions of applied magnetic field (*H*) and electric current (*I*) according to the three-dimensional Cartesian coordinate system. $H_{||y}$ and $H_{||x}$ denote the *H* applied along the *t*- and *l*-directions of the single crystal in the *y*- and *x*-axes, respectively.

^{a)}Electronic mail: eeswor@polyu.edu.hk.

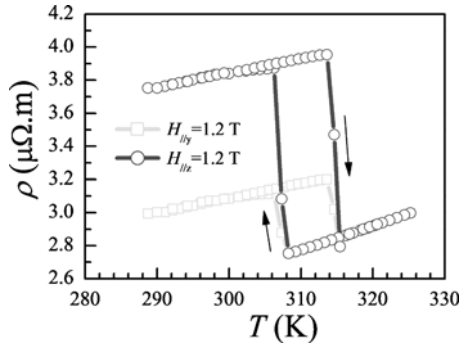


FIG. 2. (Color online) Measured electrical resistivity-temperature (ρ - T) curves at $H_{\parallel y}=1.2$ T and $H_{\parallel z}=1.2$ T during heating and cooling.

mined to be tetragonal with the lattice parameters of $a=b=0.594$ nm and $c=0.560$ nm using the x-ray diffraction technique (Bruker AXS D8 Advance) at room temperature. The electrical resistivity (ρ) as functions of H and temperature (T) were measured based on a four-electrode method with I applied along the l -direction in the z -axis using the Hall measurement method (Lakeshore 7607). In this work, two different directions of H were studied, including the one applied along the t -direction in the y -axis (denoted as $H_{\parallel y}$) and the one applied along the l -direction in the z -axis (denoted as $H_{\parallel z}$). The MR effect was evaluated from the measured ρ - H - T data using the relations $\text{MR}_p = [\rho(H_{\parallel z}) - \rho(H_{\parallel y} = 1.2 \text{ T})] / \rho(H_{\parallel y} = 1.2 \text{ T})$ and $\text{MR}_n = [\rho(H_{\parallel y}) - \rho(H_{\parallel z} = 1.2 \text{ T})] / \rho(H_{\parallel z} = 1.2 \text{ T})$ for the positive and negative MR effects, respectively (where $H=1.2$ T was used to preset an initial nearly single-variant state in the single crystal, to be addressed in Sec. III). The dependence of the MR values on the spatial angle (θ) between the directions of H and I was acquired from the ρ - H data by rotating the single crystal (also the direction of I) in the Hall measurement system at room temperature.

III. RESULTS AND DISCUSSION

Figure 2 shows the measured ρ - T curves under $H=1.2$ T applied along the t -direction in the y -axis ($H_{\parallel y}$ case) and along the l -direction in the z -axis ($H_{\parallel z}$ case) for the heating and cooling sequences. It is clear that the transition points at which ρ changes abruptly are nearly independent of the direction of H . These points can be associated with the austenite start (A_s)=314 K, austenite finish (A_f)=316 K, martensite start (M_s)=308 K, and martensite finish (M_f)=306 K, giving rise to the ρ - T hysteresis loops around the first-order martensitic-austenitic phase transformation ($T=306$ –316 K).

In details, for the martensitic phase ($T < 306$ K), there is a great difference in ρ between the $H_{\parallel y}$ and $H_{\parallel z}$ cases, while there is no observable difference in ρ for the two cases in the austenitic phase ($T > 316$ K). It is recalled that the easy crystallographic axis (or the c -axis) in the martensitic phase of Ni-Mn-Ga single crystals is always the preferential direction for H ; this assumes that if the martensitic twin variants are not locked (i.e., the magnetization vectors can rotate away from the c -axis), H (~ 1.2 T) is sufficiently large to produce a reorientation of martensitic twin variants.¹⁵ In or-

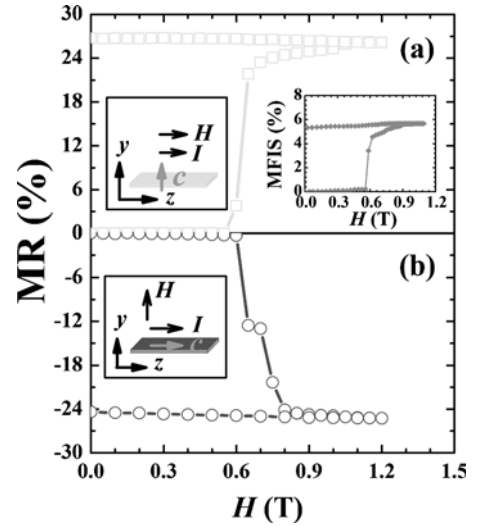


FIG. 3. (Color online) (a) Positive and (b) negative MRs as a function of applied magnetic field (H) at room temperature (298 K) based on the initial nearly single-variant states L and S preset by $H_{\parallel y}=1.2$ T and $H_{\parallel z}=1.2$ T, respectively. The inset shows the load-free dc MFIS curve of the single crystal.

der to give an insight into the influence of H on the configuration of martensitic twin variants, we have also measured the dimensional change in the single crystal in response to $H_{\parallel y}$ and $H_{\parallel z}$ at room temperature. It has been observed that the single crystal exhibits the longest dimensions of $12.150^l \times 3.061^w \times 0.485^t$ mm³ for the $H_{\parallel y}$ case and the shortest dimensions of $11.500^l \times 3.221^w \times 0.487^t$ mm³ for the $H_{\parallel z}$, giving the relative length ratio of 0.947. This ratio agrees well with the lattice c/a ratio of 0.943, indicating that the single crystal possesses two distinct nearly single-variant states, i.e., the $H_{\parallel y}$ -induced “the longest” state with the c -axis parallel to the t -direction in the y -axis (denoted as state “L”) and the $H_{\parallel z}$ -induced “the shortest” state with the c -axis parallel to the l -direction in the z -axis (denoted as state “S”). In other words, both $H_{\parallel y}$ and $H_{\parallel z}$, each having a sufficiently large magnitude of 1.2 T, are capable of presetting the two distinct initial nearly single-variant states (i.e., states L and S) in the single crystal. Therefore, the observed great difference in ρ for the martensitic phase ($T < 306$ K) between the $H_{\parallel y}$ and $H_{\parallel z}$ cases (Fig. 2) mainly originates from the electrical resistivity anisotropy.

Figure 3 shows the positive and negative MRs as a function of H at room temperature (298 K). Prior to the measurement of positive MR, an $H_{\parallel y}$ of 1.2 T was applied to preset the initial nearly single-variant state L (the longest state) with the c -axis parallel to the y -axis so that the subsequent application of H in the range of 0–1.2 T along the z -axis generates the positive MR as shown in Fig. 3(a). Similarly, the use of an $H_{\parallel z}$ of 1.2 T along the z -axis presets the initial nearly single-variant state S (the shortest state) with the c -axis parallel to the z -axis so that the subsequent application of H in the range of 0–1.2 T along the y -axis generates the negative MR as shown in Fig. 3(b).

From Figs. 3(a) and 3(b), no obvious MRs are seen for H up to ~ 0.55 T. Once H is beyond this critical value, the positive and negative MRs develop rapidly and become saturated at 26.6 and -25.2% at a moderate H of ~ 1.0 T, re-

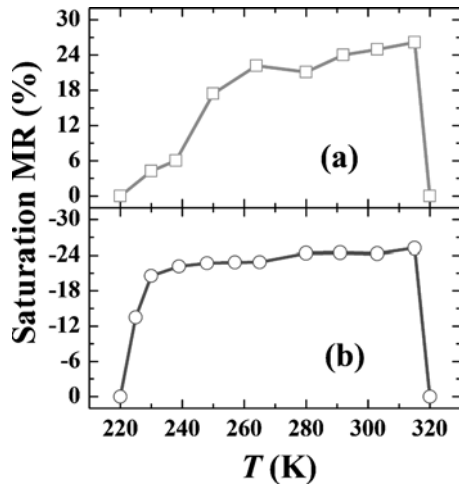


FIG. 4. (Color online) Temperature (T) dependence of (a) positive and (b) negative saturation MRs based on the initial nearly single-variant states L and S preset by $H_{||y}=1.2$ T and $H_{||z}=1.2$ T, respectively.

spectively. When H is reduced back to zero, these MR values of 26.6 and -25.2% remain almost unchanged. The slight difference in the magnitude of the two saturation MRs may be explained by the presence of different ρ in the initial nearly single-variant state L compared to the state S (Fig. 2). Nevertheless, these two MR- H curves have similar quantitative trends to the load-free dc MFIS curve caused by the reorientation of martensitic twin variants as shown in the inset of Fig. 3(a) and reported elsewhere.^{13–15} Since the observed saturation MRs are significantly larger than the maximum load-free dc MFIS of 5.6% at room temperature, it is believed that the occurrence of such large saturation MRs are mostly due to the magnetic field-induced reorientation of martensitic twin variants and the electrical resistivity anisotropy, instead of a follow-up result of the MFIS.¹⁵

Figure 4 plots the T -dependence of positive and negative saturation MRs based on the preset initial nearly single-variant states L and S, respectively. It is seen that the positive saturation MR of $\sim 26.6\%$ is developed in the T -range from 260 to 315 K, while the negative saturation MR of $\sim 25.2\%$ is formed from 230 to 315 K. For comparison, Ni–Mn–Ga alloys usually show the largest MRs during the narrow martensitic–austenitic phase transformation.^{10–12}

Figure 5 shows the saturation MR as a function of spatial angle (θ) between H and I for different magnitudes of H at

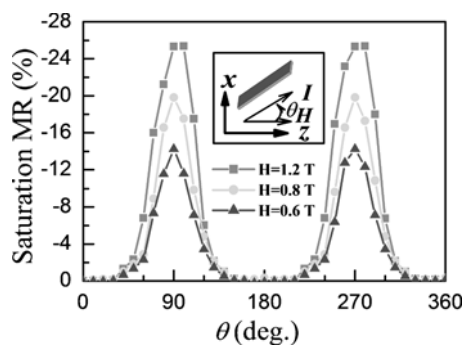


FIG. 5. (Color online) Negative saturation MR as a function of spatial angle (θ) between the directions of applied magnetic field (H) and electric current (I) for different magnitudes of H at room temperature (298 K) based on the initial nearly single-variant state S preset by $H_{||z}=1.2$ T.

room temperature (298 K) based on the preset initial nearly single-variant state S. It is noted that the direction of H was maintained along the z -axis, while that of I was kept along the l -direction of the single crystal so that θ was obtained by rotating the single crystal (also I) with respect to H . It is found that the MR value varies periodically with θ . The saturation MR has a periodic change between 0 and $\sim -25\%$ for every 180° or half cycle of θ . The reason can be explained by the periodic reorientation of the twin variants.¹⁷ Moreover, the magnitude of the MR value is controllable by H , e.g., -25.2% at $H=1.2$ T, -19.8% at $H=0.8$ T, and -14.3% at $H=0.6$ T.

IV. CONCLUSION

We have studied the MR effect in a ferromagnetic shape memory $\text{Ni}_{50}\text{Mn}_{29}\text{Ga}_{21}$ single crystal as functions of applied magnetic field, temperature, and crystallographic orientation. Interestingly large positive and negative MRs, each of $\sim 25\%$ depending on the initial state of martensitic twin variants as well as the direction and magnitude of applied magnetic field, have been observed in a wide temperature range varying about room temperature (298 K) from 230 to 315 K at a relatively small magnetic field of 1.2 T. This specific MR effect has been found to originate from the magnetic field-induced reorientation of martensitic twin variants with electrical resistivity anisotropy in the single crystal.

ACKNOWLEDGMENTS

This work was supported by the Research Grants Council of the HKSAR Government under Grant No. PolyU 5257/06E and The Hong Kong Polytechnic University under Grant No. A-PA3C.

- ¹M. N. Baibich, J. M. Broto, A. Fert, F. Nguyen Van Dau, F. Petroff, P. Eitenne, G. Creuzet, A. Friederich, and J. Chazelas, *Phys. Rev. Lett.* **61**, 2472 (1988).
- ²A. E. Berkowitz, J. R. Mitchell, M. J. Carey, A. P. Young, S. Zhang, F. E. Spada, F. T. Parker, A. Hutten, and G. Thomas, *Phys. Rev. Lett.* **68**, 3745 (1992).
- ³J. Q. Xiao, J. S. Jiang, and C. L. Chien, *Phys. Rev. Lett.* **68**, 3749 (1992).
- ⁴J. S. Moodera, L. R. Kinder, T. M. Wong, and R. Meservey, *Phys. Rev. Lett.* **74**, 3273 (1995).
- ⁵S. Jin, T. H. Tiefel, M. McCormack, R. A. Fastnacht, R. Ramesh, and L. H. Chen, *Science* **264**, 413 (1994).
- ⁶J. Mira, F. Rivadulla, J. Rivas, A. Fondado, T. Guidi, R. Caciuffo, F. Carsughi, P. G. Radaelli, and J. B. Goodenough, *Phys. Rev. Lett.* **90**, 097203 (2003).
- ⁷V. K. Sharma, M. K. Chattopadhyay, K. H. B. Shaeb, A. Chouhan, and S. B. Roy, *Appl. Phys. Lett.* **89**, 222509 (2006).
- ⁸S. Y. Yu, Z. H. Liu, G. D. Liu, J. L. Chen, Z. X. Cao, G. H. Wu, B. Zhang, and X. X. Zhang, *Appl. Phys. Lett.* **89**, 162503 (2006).
- ⁹Z. D. Han, D. H. Wang, C. L. Zhang, H. C. Xuan, J. R. Zhang, B. X. Gu, and Y. W. Du, *J. Appl. Phys.* **104**, 053906 (2008).
- ¹⁰C. Biswas, R. Rawat, and S. R. Barmana, *Appl. Phys. Lett.* **86**, 202508 (2005).
- ¹¹S. Banik, R. Rawat, P. K. Mukhopadhyay, B. L. Ahuja, A. Chakrabarti, P. L. Paulose, S. Singh, A. K. Singh, D. Pandey, and S. R. Barman, *Phys. Rev. B* **77**, 224417 (2008).
- ¹²Z. H. Liu, H. Liu, X. X. Zhang, X. K. Zhang, J. Q. Xiao, Z. Y. Zhu, X. F. Dai, G. D. Liu, J. L. Chen, and G. H. Wu, *Appl. Phys. Lett.* **86**, 182507 (2005).

- ¹³S. J. Murray, M. Marioni, S. M. Allen, R. C. O'Handley, and T. A. Lograsso, *Appl. Phys. Lett.* **77**, 886 (2000).
- ¹⁴A. Sozinov, A. A. Likhachev, N. Lanska, and K. Ullakko, *Appl. Phys. Lett.* **80**, 1746 (2002).
- ¹⁵M. Zeng, S. W. Or, and H. L. W. Chan, *J. Appl. Phys.* **107**, 09A942 (2010).
- ¹⁶V. K. Srivastava, R. Chatterjee, and R. C. O'Handley, *Appl. Phys. Lett.* **89**, 222107 (2006).
- ¹⁷P. Müllner, V. A. Chernenko, M. Wollgarten, and G. Kosterz, *J. Appl. Phys.* **92**, 6708 (2002).